

# Magnetically tunable Feshbach resonances in Li + Yb( $^3P_J$ )

Maykel L. González-Martínez and Jeremy M. Hutson\*

Joint Quantum Centre (JQC) Durham/Newcastle, Department of Chemistry,  
Durham University, South Road, Durham, DH1 3LE, United Kingdom

(Dated: March 2, 2022)

We have investigated magnetically tunable Feshbach resonances arising from the interaction of Li( $^2S$ ) with metastable Yb( $^3P_2$ ) and ( $^3P_0$ ). For Yb( $^3P_2$ ), all the resonance features are strongly suppressed by inelastic collisions that produce Yb in its lower-lying  $^3P_1$  and  $^3P_0$  states. For Yb( $^3P_0$ ), sharp resonances exist but they are extremely narrow (widths less than 1 mG).

There is currently great interest in the production of ultracold molecules, driven by potential applications in fields ranging from high-precision measurement to ultracold chemistry [1]. Many groups have succeeded in producing alkali-metal dimers in high-lying vibrational states by either magnetoassociation or photoassociation [2–4], and a few species have been transferred to their absolute ground states, either incoherently by absorption followed by spontaneous emission [5, 6] or coherently by stimulated Raman adiabatic passage (STIRAP) [7–10]. KRb molecules produced by STIRAP [8] have been used to investigate ultracold chemical reactions [11, 12] and the properties of dipolar quantum gases [12].

The alkali-metal dimers all have singlet ground states. There is great interest in extending molecule formation to molecules with doublet ground states, such as those formed from an alkali-metal or other closed-shell atom and an alkaline-earth atom. Such molecules have properties that may be important in quantum information processing [13]. Żuchowski *et al.* [14] have shown that such systems can have magnetically tunable Feshbach resonances, with the incoming channel coupled to a bound state by the very weak distance-dependence of the hyperfine coupling. The resulting Feshbach resonances are very narrow [15, 16], but nevertheless several groups have begun experiments aimed at observing them in systems such as Li+Yb [17–19] and Rb+Yb [20–22].

The Li+Yb system has particularly narrow resonances when the atoms are in their ground states. Five of the seven stable isotopes of Yb have spin-zero nuclei, and for these the resonances are predicted to be only a few  $\mu\text{G}$  wide [15]. The fermionic isotopes  $^{171}\text{Yb}$  and  $^{173}\text{Yb}$  are predicted to have somewhat wider resonances, but even these are predicted to be only around 1 mG wide [15]. However, ultracold Yb can also be prepared in its metastable  $^3P_2$  state [23], which has a radiative lifetime of at least 15 s [23, 24]. Atoms in  $P$  states are anisotropic [25], so the interaction of Yb( $^3P_2$ ) with Li( $^2S$ ) introduces several additional couplings that may be expected to produce broader resonances [26]. Hansen *et al.* [27] have suggested using these for molecule formation. If this can be achieved, it will open up a new route to the production of molecules with both electron spin and electric dipole moments, which may be applicable to a wide variety of

species. The purpose of the present paper is to investigate the feasibility of this approach.

Yb( $^3P$ ) interacts with Li( $^2S$ ) to produce four electronic states, of  $^2\Sigma^+$ ,  $^2\Pi$ ,  $^4\Sigma^+$  and  $^4\Pi$  symmetry. In the present work we have used potential curves for these states (neglecting spin-orbit coupling) calculated by Gopakumar *et al.* [28] using CASPT2 calculations (complete active space with second-order perturbation theory). These are qualitatively similar to the curves of Zhang *et al.* [29]. The two doublet states are each over  $5000\text{ cm}^{-1}$  deep, while the quartet states are shallower. The  $^2\Sigma^+$  state shows strong attraction at considerably longer range than  $^2\Pi$  because of chemical bonding involving the Li( $2s$ ) and Yb( $6p_z$ ) orbitals. We have interpolated the curves using the Reproducing Kernel Hilbert Space (RKHS) approach of Ho and Rabitz [30], and constrained them at long range to have  $C_6$  coefficients that are the same for doublet and quartet curves but different for  $\Sigma$  and  $\Pi$  curves. We obtained the value  $C_6^0 = 2312.6 E_h a_0^6$  for Li( $^2S$ ) + Yb( $^3P$ ), using Tang’s combination rule [31] with the values of the static polarizability and dispersion coefficients for Li [32] and Yb( $^3P$ ) [33]. This was interpreted as the average value,  $C_6^0 = (1/3)(C_6^\Sigma + 2C_6^\Pi)$ . The difference  $C_6^\Sigma - C_6^\Pi$  is not known for Li+Yb, so we used the approximation that the ratio  $C_6^\Sigma/C_6^\Pi$  is the same for LiYb as for LiSr, where Jiang *et al.* [34] obtained the ratio 1.146; this gives  $C_6^\Sigma = 2528$  and  $C_6^\Pi = 2205 E_h a_0^6$  for Li( $^2S$ ) + Yb( $^3P$ ). The resulting curves are shown in Fig. 1 [35].

We have carried out coupled-channel scattering calculations to characterize the magnetically tunable Feshbach resonances. The collision Hamiltonian is

$$\frac{\hbar^2}{2\mu} \left( -\frac{d^2}{dR^2} + \frac{\hat{L}^2}{R^2} \right) + \hat{H}_{\text{Li}} + \hat{H}_{\text{Yb}} + \hat{U}(R), \quad (1)$$

where  $R$  is the internuclear distance,  $\mu$  is the reduced mass, and  $\hat{L}$  is the angular momentum operator for relative motion of the two atoms. The free-atom Hamiltonians are taken to be

$$\begin{aligned} \hat{H}_{\text{Li}} &= \zeta_{\text{Li}} \hat{l}_{\text{Li}} \cdot \hat{s}_{\text{Li}} + (g_e \mu_B \hat{s}_{z,\text{Li}} + g_{\text{Li}} \mu_N \hat{l}_{z,\text{Li}}) B; \\ \hat{H}_{\text{Yb}} &= a_{\text{Yb}}^{\text{so}} \hat{l} \cdot \hat{s}_{\text{Yb}} + \left( \mu_B \hat{l}_z + g_e \mu_B \hat{s}_{z,\text{Yb}} \right) B. \end{aligned} \quad (2)$$

Here we use the convention that quantum numbers of the individual collision partners are represented by lower-case

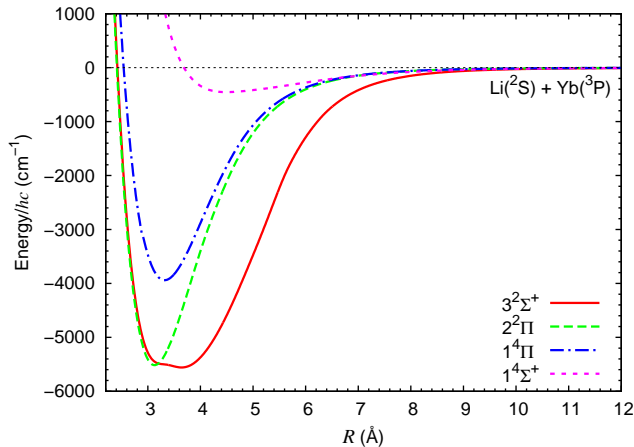


FIG. 1. Potential curves used in the present work for  $\text{Li}(^2S)$  interacting with  $\text{Yb}(^3P)$ , based on the electronic structure calculations of Gopakumar *et al.* [28].

letters, so that  $\hat{l}$  and  $\hat{s}_{\text{Yb}}$  are the orbital and electron spin angular momentum operators for the Yb atom, and  $\hat{s}_{\text{Li}}$  and  $\hat{i}_{\text{Li}}$  are the electron and nuclear spin operators for the Li atom.  $\zeta_{\text{Li}}$  is the hyperfine coupling constant for  $\text{Li}(^2S)$ ,  $a_{\text{Yb}}^{\text{so}}$  is the spin-orbit coupling constant for  $\text{Yb}(^3P)$ , and  $B$  is the magnetic field. In the present work we used  $a_{\text{Yb}}^{\text{so}} = 859.1905 \times hc \text{ cm}^{-1}$ , which gives the correct value for the splitting between the  $^3P_2$  and  $^3P_1$  states [36]. The interaction operator  $\hat{U}(R)$  may be written

$$\hat{U}(R) = \sum_{\Lambda, S} |\Lambda, S\rangle V^{\Lambda, S}(R) \langle \Lambda, S | + \hat{V}^{\text{d}}(R), \quad (3)$$

where  $\Lambda = 0$  and 1 indicates the  $\Sigma$  and  $\Pi$  states,  $S = 1/2$  and  $3/2$  is the total electron spin (for the doublet and quartet potentials, respectively), and  $\hat{V}^{\text{d}}(R)$  represents the dipolar interaction between the magnetic moments due to Li and Yb unpaired electrons.

We have implemented this Hamiltonian in the BOUND program for calculating bound-state energies [37] and the MOLSCAT scattering package [38], using two different basis sets:  $|l s_{\text{Yb}} j m_j\rangle |s_{\text{Li}} m_{s, \text{Li}}\rangle |i_{\text{Li}} m_{i, \text{Li}}\rangle |LM_L\rangle$  and  $|l m_l s_{\text{Yb}} m_{s, \text{Yb}}\rangle |s_{\text{Li}} m_{s, \text{Li}}\rangle |i_{\text{Li}} m_{i, \text{Li}}\rangle |LM_L\rangle$ . Here  $j = 0, 1$  or 2 is the total angular momentum of Yb and the  $m$  and  $M$  quantum numbers are angular momentum projections onto the axis of the applied magnetic field. The only rigorously conserved quantities are the projection of the total angular momentum,  $M_{\text{tot}} = m_j + m_{s, \text{Li}} + m_{i, \text{Li}} + M_L = m_l + m_{s, \text{Yb}} + m_{s, \text{Li}} + m_{i, \text{Li}} + M_L$  and total parity  $P = (-1)^{L+1}$ . We have verified that the two basis sets give identical results when all possible values of  $j$  and the projection quantum numbers for a given  $M_{\text{tot}}$  are included. However, the first of the two basis sets has the advantage that it is possible to restrict the basis functions to those correlating with an individual spin-orbit state of Yb, which will be important in the discussion below.

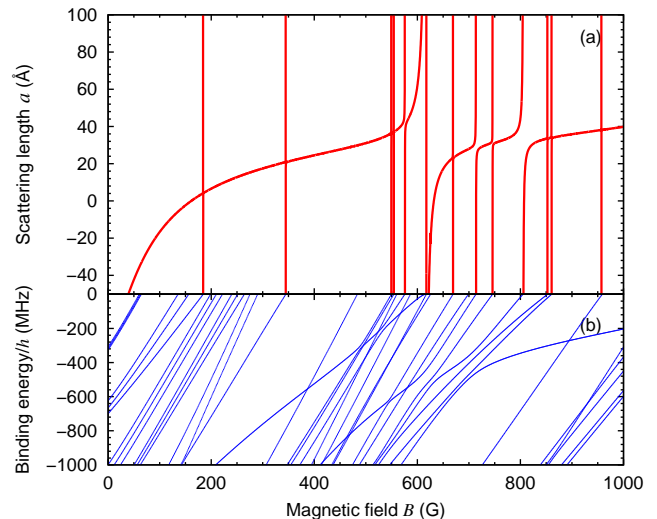


FIG. 2. (a) Scattering length  $a(B)$  for collisions of Li in its absolute ground state with  $\text{Yb}(^3P_2, m_j = -2)$ , including only Yb basis functions with  $j = 2$ . (b) The near-threshold bound states responsible for the resonances in (a).

We first consider calculations for  $\text{Li}(^2S) + \text{Yb}(^3P_2)$  with both  $^6\text{Li}$  and  $^{174}\text{Yb}$  in their lowest Zeeman state ( $f = 1/2, m_f = 1/2$  for Li and  $m_j = -2$  for Yb), restricting the basis set to functions with  $j = 2$ . Convergence was achieved with  $L_{\text{max}} = 12$ . Fig. 2(a) shows the resulting s-wave scattering length  $a(B)$ , calculated at a collision energy of  $100 \text{ nK} \times k_{\text{B}}$ , as a function of magnetic field  $B$ . It may be seen that there are numerous resonances with widths in the range 0.1 to 10 G, which at first sight look promising candidates for molecule formation. Fig. 2(b) shows the near-threshold bound states calculated with the same basis set. It may be seen that only a small fraction of the bound states that cross threshold cause visible resonances; the widest resonances are due to bound states that are dominated by low  $L$  quantum numbers.

The promising results shown in Fig. 2 unfortunately neglect couplings to the lower-lying  $^3P_0$  and  $^3P_1$  states of Yb. It is known that Feshbach resonances in the presence of inelastic scattering have signatures that are no longer pole-like, but instead exhibit more complicated lineshapes in which the poles are suppressed [39]. The scattering length in the presence of inelastic scattering is complex,  $a(B) = \alpha(B) - i\beta(B)$ , where  $\beta(B)$  represents a 2-body inelastic loss rate  $k_{\text{loss}} \approx 4\pi\hbar\beta(B)/\mu$ . We have therefore repeated the scattering calculations for  $\text{Li} + \text{Yb}(^3P_2, m_j = -2)$ , including the  $^3P_0$  and  $^3P_1$  basis functions, and produced the scattering length and loss rate shown as red curves in Fig. 3. It may be seen that the inelastic processes have greatly reduced the amplitude of the oscillations in  $a(B)$  and produced fast loss rates over most of the range of magnetic field considered. Such fast loss rates are likely to prevent the use of these

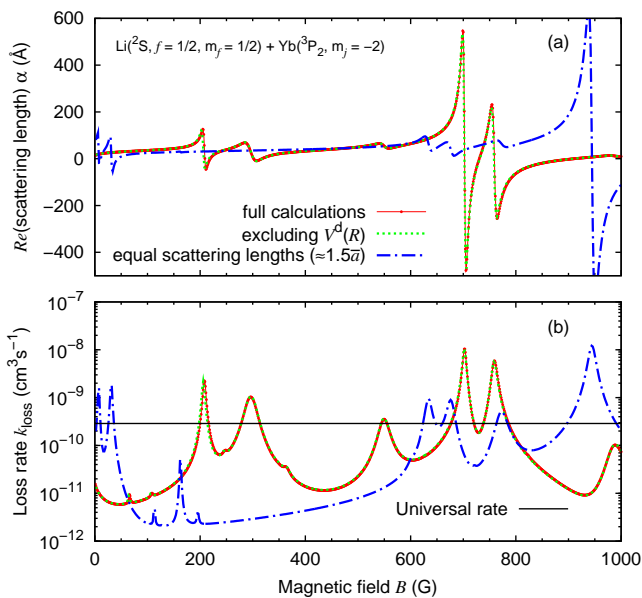


FIG. 3. (a) The real part  $\alpha(B)$  of the scattering length for collisions of Li in its absolute ground state with  $\text{Yb}(^3P_2, m_j = -2)$ , including Yb basis functions with  $j = 0, 1$  and  $2$ . (b) The corresponding 2-body loss rate  $k_{\text{loss}}$ .

resonances for molecule formation.

The loss rates shown in Fig. 3 are generally lower than the “universal” loss rate predicted by Idziaszek and Julienne [40] for systems in which all collisions that reach short range produce inelasticity, which is  $2.9 \times 10^{-10} \text{ cm}^3 \text{ s}^{-1}$  in the present case, shown by the horizontal black line in Fig. 3. However, they are considerably faster than those observed experimentally for  $\text{Yb}(^3P_2, m_j = -2) + \text{Yb}(^1S_0)$  [41], which are below  $10^{-12} \text{ cm}^3 \text{ s}^{-1}$  at fields up to 1 G. Interestingly, repeating the Li+ $\text{Yb}(^3P_2, m_j = -2)$  calculations with the Li spins set to zero also produces much lower loss rates, below  $10^{-12} \text{ cm}^3 \text{ s}^{-1}$  except near narrow resonances using the doublet potential curves, and even lower using the less anisotropic quartet potentials. This makes it clear that the *difference* between the doublet and quartet potentials, which can drive spin exchange processes, is key in causing the fast loss rates.

It should be emphasized that the inelastic transitions from the  $j = 2, m_j = -2$  state are driven principally by the Born-Oppenheimer potentials of Fig. 1 and *not* to any great extent by the magnetic dipolar interaction  $V^d(R)$ . To demonstrate this we have repeated the calculation with the magnetic dipolar term omitted, and obtained the results shown as dotted green curves in Fig. 3. These differ only slightly from the results with  $V^d(R)$  included. When states of  $\Sigma$  and  $\Pi$  character both exist and have different potential curves, the difference may be viewed as an “anisotropy” in the interaction, and produces matrix elements off-diagonal in both  $j$  and  $m_j$ .

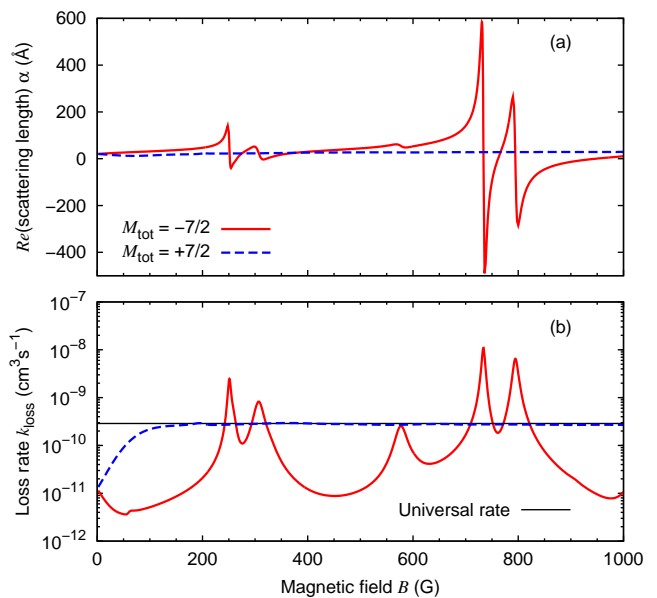


FIG. 4. (a) The real part  $\alpha(B)$  of the scattering length for spin-stretched collisions of Li and  $\text{Yb}(^3P_2)$ ,  $M_{\text{tot}} = -7/2$  and  $M_{\text{tot}} = +7/2$ , including Yb basis functions with  $j = 0, 1$  and  $2$ . (b) The corresponding two-body loss rates  $k_{\text{loss}}$ .

In the present case, the state-to-state cross sections for formation of  $\text{Yb}(^3P_1)$  are approximately a factor of 100 larger than those for formation of  $\text{Yb}(^3P_0)$ .

We have also investigated resonances for spin-stretched collisions,  $\text{Yb}(^3P_2, m_j = -2) + \text{Li}(m_f = -3/2)$  ( $M_{\text{tot}} = -7/2$ ) and  $\text{Yb}(^3P_2, m_j = +2) + \text{Li}(m_f = +3/2)$  ( $M_{\text{tot}} = +7/2$ ). The results are shown in Fig. 4. The results for  $M_{\text{tot}} = -7/2$  are remarkably similar to those for  $M_{\text{tot}} = -3/2$  in Fig. 2, with just a small shift in field: the  $-3/2$  and  $-7/2$  thresholds are close in energy (within 200 MHz), the resonances are caused by the same bound states, and the principal loss mechanism (formation of  $\text{Yb}(^3P_1)$ ) is the same. For  $M_{\text{tot}} = +7/2$ , by contrast, spin relaxation to form lower-lying Zeeman states of  $\text{Yb}(^3P_2)$  is the dominant mechanism. These spin relaxation processes are so fast that the loss rate is very close to the “universal” rate at fields above 100 G. The situation is thus quite different from that for the alkali-metal pairs, where inelastic processes are strongly suppressed for spin-stretched collisions. The difference arises because, for the alkali-metal pairs, the interaction potential is isotropic and only the magnetic dipole interaction can cause spin relaxation. In the present case, by contrast, changes in  $j$  and  $m_j$  can be driven directly by the anisotropic interaction potentials.

The potential energy curves of Gopakumar *et al.* [28] are likely to be qualitatively correct, but they are unlikely to be accurate enough to predict the correct values of the four scattering lengths. However, the overall density of levels is controlled by the  $C_6$  coefficient, and (no

matter what the scattering length), every threshold supports an s-wave bound state within approximately 7 GHz of threshold. There are also higher- $L$  states supported by these and deeper levels. As may be seen in Fig. 2, the bound states are actually well distributed across this range, and many of them cross the  $m_j = -2$  threshold at fields below 1000 G. The potentials we have used should therefore reliably predict the overall *density* of Feshbach resonances, but will not give quantitative predictions of their positions and widths.

It is important to consider whether the potential curves will accurately predict the *strength of decay* and hence the extent of the suppression of the peaks in the scattering length. In particular, for the alkali-metal dimers it is known that the rate of inelastic (spin exchange) collisions depends strongly on the *difference* in scattering lengths between the singlet and triplet states [42], and that inelastic rates can be anomalously low when the singlet and triplet scattering lengths are very similar. The particular potential curves used in Fig. 2 have scattering lengths of  $-89.27$  and  $50.30 a_0$  for the  $^2\Sigma^+$  and  $^4\Sigma^+$  states and  $58.30$  and  $90.82 a_0$  for the  $^2\Pi$  and  $^4\Pi$  states. In order to estimate whether an analogous effect may reduce the loss rates in  $\text{Li} + \text{Yb}(^3P_2)$ , we have investigated an artificial problem in which the potentials are adjusted so that all four scattering lengths have the same value,  $57.75 a_0$ , chosen to be approximately 1.5 times the mean scattering length  $\bar{a}$  [43], which is about  $40 a_0$  for this system. The results are shown as blue dot-dashed curves in Fig. 3; the resonances are of course in different locations, but the degree of damping is comparable. This demonstrates that equal scattering lengths are not sufficient to suppress inelasticity in the present case. The suppression observed for spin exchange in  $^{87}\text{Rb}$  in ref. [42] was for inelastic collisions involving two near-threshold channels, where similar scattering lengths implied similar long-range wavefunctions. In the present case, with a large kinetic energy release, the long-range wavefunctions are quite different even when the scattering lengths are the same.

We have also explored whether the  $^3P_0$  metastable state of Yb offers the possibility of broad Feshbach resonances. This state has a radiative lifetime that is of order 20 s for  $^{171}\text{Yb}$  and  $^{173}\text{Yb}$  [44–46] and is too long to be observed without an applied field for bosonic Yb isotopes [47]. The near-threshold bound states that might cause resonances at this threshold (with Li in its absolute ground state) are shown as red lines in Fig. 5. There are bound states that cross threshold as a function of magnetic field, arising from states in which the Li is in a higher magnetic or hyperfine state. For the potentials considered here, the states that cross threshold have  $L = 4$ . They are coupled to the incoming s-wave channel only by the spin dipolar term, acting in second order, or indirectly by the potential anisotropy via the far-away  $^3P_1$  and  $^3P_2$  states. The resulting Feshbach res-

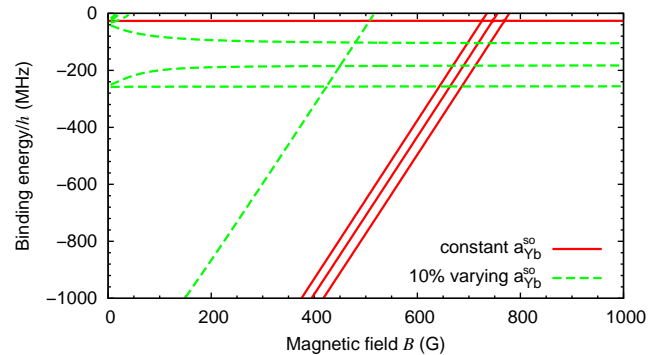


FIG. 5. Near-threshold bound states relative to the absolute ground state  $\text{Li} + \text{Yb}(^3P_0)$  threshold, with the spin-orbit coupling constant held fixed at its atomic value (solid, red) and allowed to vary by 10% across the range of chemical interactions (dashed, green).

onances are so narrow that we were unable to locate them in scattering calculations.

The interaction operator (3) does neglect some terms. In particular, it neglects the  $R$ -dependence of the spin-orbit coupling operator. This might in principle introduce stronger coupling between the bound and continuum states, in the same way as the  $R$ -dependence of the hyperfine coupling in systems such as  $\text{RbSr}$  [14] and alkali metal +  $\text{Yb}(^1S)$  [15, 16]. We have therefore repeated the calculations introducing an  $R$ -dependent spin-orbit coupling  $a_{\text{Yb}}^{\text{so}}(R)$  that varies by up to 20% of its value across the well region, with a shape obtained by scaling the electronic structure calculations of Gopakumar *et al.* [28]. The bound states for a 10% change are shown as dashed green lines in Fig. 5; they naturally shift in position, but the couplings between the bound states and the incoming wave are not significantly larger and we were again unable to identify Feshbach resonances in scattering calculations. The mechanism that produces Feshbach resonances for  $\text{Li} + \text{Yb}(^1S)$ , through the  $R$ -dependence of the Li hyperfine coupling [15], will still exist for  $\text{Yb}(^3P_0)$ , but it nevertheless appears that resonances at the  $^3P_0$  threshold are not significantly wider than those for the ground state.

We thus conclude that Feshbach resonances arising from interaction of any atom in a  $^3P_2$  state with an alkali-metal atom are likely to be strongly decaying, provided that the  $^3P_0$  and  $^3P_1$  states lie below the  $^3P_2$  state. Resonances that occur at the  $^3P_0$  threshold are extremely narrow.

[Note: We are aware that the group at Temple University [48] is carrying out a parallel investigation into  $\text{Li} + \text{Yb}$  resonances at the  $\text{Yb}(^3P_2)$  threshold.]

The authors are grateful to EPSRC and EOARD for funding.

- 
- \* J.M.Hutson@durham.ac.uk
- [1] L. D. Carr, D. DeMille, R. V. Krems, and J. Ye, *New J. Phys.* **11**, 055049 (2009).
  - [2] J. M. Hutson and P. Soldán, *Int. Rev. Phys. Chem.* **25**, 497 (2006).
  - [3] T. Köhler, K. Goral, and P. S. Julienne, *Rev. Mod. Phys.* **78**, 1311 (2006).
  - [4] K. M. Jones, E. Tiesinga, P. D. Lett, and P. S. Julienne, *Rev. Mod. Phys.* **78**, 483 (2006).
  - [5] J. M. Sage, S. Sainis, T. Bergeman, and D. DeMille, *Phys. Rev. Lett.* **94**, 203001 (2005).
  - [6] J. Deiglmayr, A. Grochola, M. Repp, K. Mörtlbauer, C. Glück, J. Lange, O. Dulieu, R. Wester, and M. Weidemüller, *Phys. Rev. Lett.* **101**, 133004 (2008).
  - [7] F. Lang, K. Winkler, C. Strauss, R. Grimm, and J. Hecker Denschlag, *Phys. Rev. Lett.* **101**, 133005 (2008).
  - [8] K.-K. Ni, S. Ospelkaus, M. H. G. de Miranda, A. Pe'er, B. Neyenhuis, J. J. Zirbel, S. Kotochigova, P. S. Julienne, D. S. Jin, and J. Ye, *Science* **322**, 231 (2008).
  - [9] J. G. Danzl, M. J. Mark, E. Haller, M. Gustavsson, R. Hart, J. Aldegunde, J. M. Hutson, and H.-C. Nägerl, *Nature Phys.* **6**, 265 (2010).
  - [10] K. Aikawa, D. Akamatsu, M. Hayashi, K. Oasa, J. Kobayashi, P. Naidon, T. Kishimoto, M. Ueda, and S. Inouye, *Phys. Rev. Lett.* **105**, 203001 (2010).
  - [11] S. Ospelkaus, K.-K. Ni, D. Wang, M. H. G. de Miranda, B. Neyenhuis, G. Quémener, P. S. Julienne, J. L. Bohn, D. S. Jin, and J. Ye, *Science* **327**, 853 (2010).
  - [12] K.-K. Ni, S. Ospelkaus, D. Wang, G. Quémener, B. Neyenhuis, M. H. G. de Miranda, J. L. Bohn, J. Ye, and D. S. Jin, *Nature* **464**, 1324 (2010).
  - [13] A. Micheli, G. K. Brennen, and P. Zoller, *Nature Phys.* **2**, 341 (2006).
  - [14] P. S. Żuchowski, J. Aldegunde, and J. M. Hutson, *Phys. Rev. Lett.* **105**, 153201 (2010).
  - [15] D. A. Brue and J. M. Hutson, *Phys. Rev. Lett.* **108**, 043201 (2012).
  - [16] D. A. Brue and J. M. Hutson, *Phys. Rev. A* **87**, 052709 (2013).
  - [17] M. Okano, H. Hara, M. Muramatsu, K. Doi, S. Uetake, Y. Takasu, and Y. Takahashi, *Appl. Phys. B* **98**, 691 (2009).
  - [18] A. H. Hansen, A. Y. Khramov, W. H. Dowd, A. O. Jamison, V. V. Ivanov, and S. Gupta, *Phys. Rev. A* **84**, 011606 (2011).
  - [19] V. V. Ivanov, A. Y. Khramov, A. H. Hansen, W. H. Dowd, F. Münchow, A. O. Jamison, and S. Gupta, *Phys. Rev. Lett.* **106**, 153201 (2011).
  - [20] F. Baumer, F. Münchow, A. Görlitz, S. E. Maxwell, P. S. Julienne, and E. Tiesinga, *Phys. Rev. A* **83**, 040702 (2011).
  - [21] F. Münchow, C. Bruni, M. Madalinskia, and A. Görlitz, *Phys. Chem. Chem. Phys.* **13**, 18734 (2011).
  - [22] F. Münchow, *2-photon photoassociation spectroscopy in a mixture of Ytterbium and Rubidium*, Ph.D. thesis, Heinrich-Heine-Universität, Düsseldorf (2012).
  - [23] A. Yamaguchi, S. Uetake, D. Hashimoto, J. M. Doyle, and Y. Takahashi, *Phys. Rev. Lett.* **101**, 233002 (2008).
  - [24] A. P. Mishra and T. K. Balasubramanian, *J. Quant. Spectrosc. Rad. Transf.* **69**, 760 (2001).
  - [25] R. H. G. Reid and A. Dalgarno, *Phys. Rev. Lett.* **22**, 1029 (1969).
  - [26] R. V. Krems, G. C. Groenenboom, and A. Dalgarno, *J. Phys. Chem. A* **108**, 8941 (2004).
  - [27] A. H. Hansen, A. Y. Khramov, W. H. Dowd, A. O. Jamison, B. Plotkin-Swing, R. J. Roy, and S. Gupta, *Phys. Rev. A* **87**, 013615 (2013).
  - [28] G. Gopakumar, M. Abe, B. P. Das, M. Hada, and K. Hirao, *J. Chem. Phys.* **133**, 124317 (2010).
  - [29] P. Zhang, H. R. Sadeghpour, and A. Dalgarno, *J. Chem. Phys.* **133**, 044306 (2010).
  - [30] T. S. Ho and H. Rabitz, *J. Chem. Phys.* **104**, 2584 (1996).
  - [31] K. T. Tang, *Phys. Rev.* **177**, 108 (1969).
  - [32] A. Derevianko, S. G. Porsev, and J. F. Babb, *Atomic Data and Nuclear Data Tables* **96**, 323 (2010).
  - [33] V. A. Dzuba and A. Derevianko, *J. Phys. B* **43**, 074011 (2010).
  - [34] J. Jiang, Y. Cheng, and J. Mitroy, arXiv:1303.1234 (2013).
  - [35] To obtain smooth curves with the correct long-range behavior, we omitted *ab initio* points outside  $R = 13.0, 8.6, 9.6$  and  $8.6 a_0$  for the  $^2\Sigma^+$ ,  $^2\Pi$ ,  $^4\Sigma^+$  and  $^4\Pi$  curves, respectively, and between  $9.6$  and  $10.5 a_0$  for the  $^2\Sigma^+$  curve.
  - [36] W. F. Meggers and J. L. Tech, *J. Res. Natl. Bur. Stand. (U.S.)* **83**, 13 (1978).
  - [37] J. M. Hutson, (2011), BOUND computer code.
  - [38] J. M. Hutson and S. Green, *MOLSCAT computer program, version 14* (CCP6, Daresbury, 1994).
  - [39] J. M. Hutson, *New J. Phys.* **9**, 152 (2007).
  - [40] Z. Idziaszek and P. S. Julienne, *Phys. Rev. Lett.* **104**, 113202 (2010).
  - [41] S. Uetake, R. Murakami, J. M. Doyle, and Y. Takahashi, *Phys. Rev. A* **86**, 032712 (2012).
  - [42] P. S. Julienne, F. H. Mies, E. Tiesinga, and C. J. Williams, *Phys. Rev. Lett.* **78**, 1880 (1997).
  - [43] G. F. Gribakin and V. V. Flambaum, *Phys. Rev. A* **48**, 546 (1993).
  - [44] S. G. Porsev, A. Derevianko, and E. N. Fortson, *Phys. Rev. A* **69**, 021403 (2004).
  - [45] C. W. Hoyt, Z. W. Barber, C. W. Oates, T. M. Fortier, S. A. Diddams, and L. Hollberg, *Phys. Rev. Lett.* **95**, 083003 (2005).
  - [46] T. Hong, C. Cramer, E. Cook, W. Nagourney, and E. N. Fortson, *Opt. Lett.* **30**, 2644 (2005).
  - [47] Z. W. Barber, C. W. Hoyt, C. W. Oates, L. Hollberg, A. V. Taichenachev, and V. I. Yudin, *Phys. Rev. Lett.* **96**, 083002 (2006).
  - [48] S. Kotochigova, (2013), private communication.